The United Nations University

GEOTHERMAL TRAINING PROGRAMME
Orkustofnun, Grensásvegur 9,
IS-108 Reykjavík, Iceland

Reports 1996
Number 17

CHEMISTRY OF THERMAL WATERS IN THE AREA FROM QUANGNAM-DANANG TO BARIA-VUNGTAU, VIETNAM

Tran Trong Thang
Research Institute of Geology and Mineral Resources,
Thanh Xuan-Dong Da-Hanoi,
VIETNAM

ABSTRACT

The results of previous investigations in Vietnam have revealed a geothermal origin for, and the possible exploitation potential of several springs in Central and South Vietnam. Seventy hot springs were sampled and then twenty-four samples selected for further study with the aim of evaluating and interpreting their chemical composition using methods such as triangular diagrams, plots of log Q/K vs. temperature and mixing models using SiO_2 content and heat content. It is indicated that the thermal springs are peripheral waters, except for two (M13 and M14 near Tuwoka) which are mature waters. According to the enthalpies obtained, the hot springs can be divided into two groups, low-enthalpy springs with geothermometer temperatures <125°C and intermediate-enthalpy springs with geothermometer temperatures between 125 and 150°C. The highest temperature predicted for a single hot spring is 144°C (sample M13).

1. INTRODUCTION

There are more than 300 thermal springs in Vietnam, with measured surface temperatures ranging from 30 to 103°C. Seventy of them are in the territory stretching from Quangnam-Danang in the north to Baria-Vungtau provinces in the south (Figure 1) with temperatures ranging from 35 to 85°C.

According to a geochemical study of twenty-three thermal springs in this area, conducted by Gianelli et al. (1996), the reservoir temperatures could be up to 150°C. Also, Quy (1996) has published a project report on mapping and assessment of geothermal potential of this territory and its prospects, in which he suggests that there exist in this area geothermal systems of low enthalpy (<125°C) and intermediate enthalpy (125-225°C).

Analytical results for twenty-four hot water samples, selected from seventy thermal springs sampled in the project area, were used. The author wanted to better clarify the chemical features of the thermal waters and recommend how detailed exploration for geothermal potential in the area should be carried out.

2. GEOLOGY AND TECTONICS OF THE RESEARCH AREA

In Southeast Asia, Vietnam is located in the southern part of the Eurasian continental plate and occupies a major portion of the Indochina peninsula. Vietnam lies along the suture between two major tectonic belts:

The Mediterranean belt, which runs through Tibet and then through Central Vietnam in a NW-SE direction from the Songma watershed through the Tamky-Phuocson area.

The Pacific belt in Southeast Asia comprises the Japan Archipelago and the southern part of Central Vietnam in a NE-SW direction. The Pacific belt in Vietnam is also referred to as the plutonic volcanic belt composed of plutonic and volcanic rock of early Mesozoic to Cenozoic age.

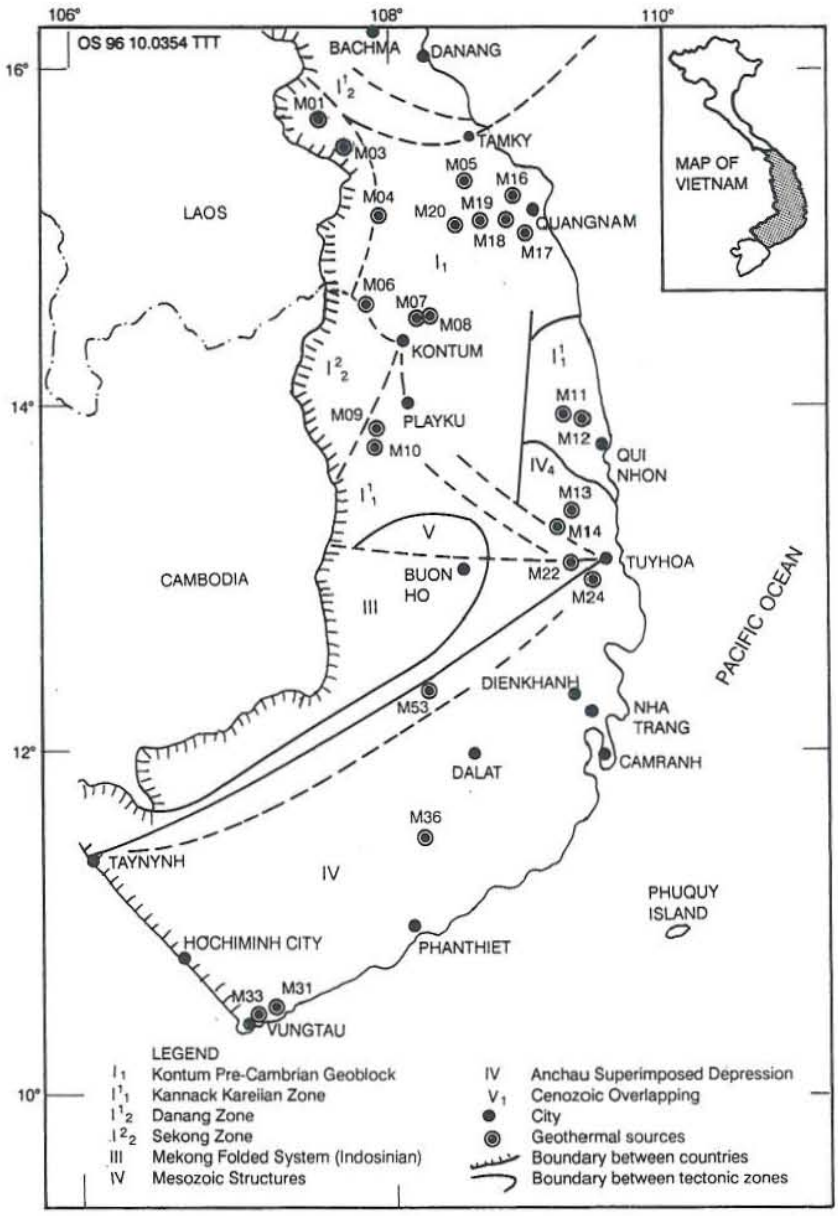

FIGURE 1: Geothermal activity and the main geological structures of the area between Quangnam-Danang and Baria-Vungtau

The northern part of the Duonglu platform is pre-Riphean in age. Its southeastern extent is referred to as the Vietnam-China folded region (early to middle Paleozoic) consisting of Southeast China and North Vietnam. The Songma zone is bounded by the Vietnam-Laos folded region (middle to late Paleozoic). The Indonesian geoblock in this region comprises, notably: 1) the uplifting Kontum geoblock the older pre-Riphean small continent consisting of the Kannak zone, which contains the Endeerbite and Chanokite formations of Archeanozoic age, and consolidated in Karalian; and 2) the Ngoclinh, which contains magmatic-metamorphic formations consolidated in Baicalian (Tri et al., 1986).

In Southwest Vietnam lies the Indochina early Mesozoic folded region (Triassic). This region stretches from Tibet through Thailand to East Malaysia. It consists of the Mekong subregion from North Laos to South Vietnam, a Cretaceous-Paleocene region from

Myamar to Himalaya and the Neogene region from Himalaya through North Kalimantan upwards to the Philippine Archipelago. Its eastern flank is a marginal sea structure occupying almost the entire east sea area along with the Spratly, which can be considered a microcontinent.

According to geothermal study results from Nghiep (1986), Vietnam can be divided into six geothermal regions on the basis of distribution of geological-tectonic zones belonging to various tectonic regions. Each geothermal region consists of many tectonic zones, which are located in different tectonic regions; thermal sources which depend strongly on neotectonic activity have controlled the emergence of geothermal sources observed in the tectonic zones.

The study area is located in the South Central Vietnam geothermal region (Figure 1). From our point of view, this region occupies an area from Quangnam-Danang to Baria-Vungtau Provinces. It consists of many tectonics zones overlapping each other and it has a very complicated geological history with extensive tectonic and magmatic activity and a prevalence of recent basaltic eruptions. With regard to geology and tectonics, the region is composed of the following zones:

The Kontum geoblock (I_1). A Pre-Cambrian continental block, it is the most ancient crystalline basement of Vietnam. It is bounded by the Tamky-Phuocson suture zone (ancient subduction zone) in the north and by the Sekong zone in the west. In the south it is overlapped by newer complexes of the Indonesian centre (for example, the Ankhe superimposed depression was filled up with continental sediments and Neogene-Quaternary basaltic effusive). The Kontum geoblock consists mainly of two zones: 1) The Kannak, composed of Archaeozoic and Endeerbite rocks and consolidated in Karalian; 2) The Ngocling, made up of Proterozoic formations and consolidated in Baicalian.

The Danang zone (I^1_2). The north part of the zone is a structural strip, which belongs to the sedimentary-volcanic complex and organic granitoid of middle Paleozoic age. This strip is distributed from offshore Danang (the Sontra peninsula) through Dailoc, and continues to the common border with Laos. The southern part is the Tamky-Phuocson suture zone. The Nongson graben sits between the above zones and was formed by tectonic activity. It was filled up with volcano clastic and coal-bearing sediments (Triassic). This zone has been controlled by the sub-parallel fault system.

The Sekong zone (I^2_2). Located west of Kontum, this zone originated from the destruction of the western edge of the Kontum geoblock and filled up with complexes of volcanic and terrigenous-tuffaceous sediments, interrelated with beds of silica, andesite and dacite. It lies along the Vietnam-Laos border and expands to the Songsekong watershed. This zone has been controlled by the sub-meridian fault system (the Pako Fault). South of the two zones is the Srepok zone in the southwest.

The Seprok zone. This is bounded in the south by the Sekong zone and the Kontum geoblock via the Buonho-Tuyhoa suture zone. The distribution area of the zone is covered up with Mesozoic formations so the outcropping area of the late Paleozoic formations has not been extensively studied to the southwest of the Hongom peninsula and on the islands in the western part of Southern Vietnam. In the Random area, there are volcanic effusive formations accompanied by siliceous shales, interbedded with sandstone and andesite tuff and interrelated with lenses of marl and andesite of Carboniferous-Pennian age.

The Dalat plutonic-volcanic zone. Located adjacent to the southern margin of the Kontum block and southeast of the Srepok zone via the Tayninh-Tuyhoa zone, this zone lies on the ancient basement of the southern Kontum edge. Terrigenous and volcanic formations (middle Triassic), such as rhyolite-dacite associated with shallow-seated porphyritic granite and dykes, are extensively developed in the zone. These formations are overlapped with terrigenous formations interrelated with andesite-dacite of the Jurassic-Cretaceous age. Many granodiorite-granite-granosyenite bodies were discovered here. The zone is controlled by the NE-SW faults. This direction is the main structural zone, which is nearly

perpendicular to the structures belonging to other structural zones of the entire region. The Dalat zone is considered to be a part of an active continental margin of "Andes type" in Southeast Asia. The western edge of the zone overlaps with a basaltic volcanic arch (Neogene-Quaternary) and the southern one is superimposed with Cenozoic unconsolidated sediment. The NE-SW fault systems are considered to be the canals for convective heat flow. Recent volcanic activity in the region is worth mentioning, for instance, the volcanic-mud eruption in Phutue (Phuyen Province) and the volcanic-ash eruption in Lave, Chuplong area that took place in February 1993. There was a basaltic eruption in Catwic Island in 1978.

3. CHEMISTRY AND ANALYTICAL METHODS

3.1 Sampling and analytical methods

The water samples were collected in several fractions. Ru samples are raw and untreated for analysis of SiO_2. Seven samples were diluted with distilled water in the proportion 1:10 (Rd). Fu are filtered and untreated samples to be used for analysis of anions. Fa samples are filtered and acidified with 1 ml "suprapur" HNO_3 added to 500 ml sample for metal element analysis. The measurements of pH, flowrate and temperature were carried out in the field. A fortnight after the field survey, all the samples were transported to the laboratory. The methods usually applied to analyse such samples are described in Table 1.

TABLE 1: Analytical laboratory methods for the chemical samples

Constituent	Sample fraction	Method	Technique
K, Na	Fa	Atomic absorption spectroscopy	Flame, Cs added
Ca, Mg	Fa	Atomic absorption spectroscopy	Flame, La added
Al	Fa	Fluorimetry/atomic absorption spectroscopy	Lumogallion/graphite furnace
Li	Fa	Atomic absorption spectroscopy	Flame
Fe, Pb	Fa	Atomic absorption spectroscopy	
As	Fa	Atomic absorption spectroscopy	Hydride generation
B	Fu	Spectrophotometry	Azomethin H
SiO_2	Rd	Spectrophotometry	Ammonium molybdate
SO_4	Fu	Ion chromatography	Conductivity detector
CO_3	Ru	Titration	pH, glass electrode
HCO_3	"	-- " --	-- " --
Cl	Fu	Titration/ion chromatography	$AgNO_3$/conductivity detector
TDS	Fu	Gravimetric	Sample evaporated and dried

3.2 Water chemistry

All samples were collected from thermal springs with artesian flowrates ranging from 0.2-28 l/s. The temperatures measured during collection of water samples ranged from 31 to 85°C. The pH is neutral or slightly acid. All the analytical results are presented in Table 2. The TDS of the samples can be divided into two groups, the first group in the range of 300-700 mg/kg, and the second 1400-1700 mg/kg. The ionic balances for the samples calculated by the WATCH program (Arnórsson et al., 1982; Bjarnason, 1994) gave values ranging from -0.33-19.3 (Table 3), which are acceptable for equilibrium calculations; the data could be used for interpretation.

TABLE 2: The chemical composition of thermal springs (in mg/kg) in the area from Quangnam-Danang to Baria-Vungtau, Vietnam

No.	Sample	pH	Surf. temp. (°C)	Flowrate (l/s)	K	Na	Ca	Mg	Al	Li	Fe	Pb	As	B	SiO_2	SO_4	CO_3	HCO_3	CL	TDS
1	M01	6	49	2	3.02	69.05	1.46	0.8	0.142	0.049	0.108	0.005	4E-04	0.044		49.77	72	147.7	53.25	1401
2	M03	7	43.2	3	3.73	109.5	4.03	0.94	0.168	0.249	0.128	9E-04	7E-04	0.187		25.01	73.5	152.1	120.7	526.6
3	M04	7	50	3	4.71	98.81	3.58	0.74	0.168	0.139	0.154	0.009	8E-04	0.033		25.01	78	162.7	96.85	492.8
4	M05	6.5	37.5	0.4	2.82	78.57	23.52	2.15	0.168	0.025	0.124	0.006	5E-04	0.01		114.4	54	110.4	65.87	516.1
5	M06	6	58	0.2	5.87	123.8	86.5	3.36	0.168	0.078	0.12	0.004	8E-04	0.016		294.7	28.5	57.61	76.33	719.5
6	M07	6.8	65	3.5	2.98	76.19	2.91	0.8	0.101	0.131	0.064	0.001	5E-04	0.008	85.26	40.02	52.5	117.2	33.72	377.3
7	M08	5.5	31	0.1	2.77	77.38	3.02	0.8	0.168	0.133	0.154	0.008	1E-04	0.059		90.04	48	97.83	49.7	444.6
8	M09	7	54	0.8	6.18	103.4	5.6	1.68	0.101	0.078	0.056	0.001	9E-04	0.011	80.95	57.81	63	129.1	60.35	468
9	M10	7	65	1	6.93	109.5	5.7	0.6	0.168	0.104	0.05	0.009	8E-04	0.009	93.88	131.9	72	150.1	23.7	546.7
10	M11	7	85	2.4	6.09	135.8	3.52	0.71	0.28	0.14	0.078	0.002	7E-04	0.07	103.18	32.45	59.75	148.9	121.8	524.6
11	M12	7	78	0.35	4.18	117.3	2.24	0.34	0.156	0.089	0.044	0.001	8E-04	0.035		25.01	76.5	159.1	74.55	450.6
12	M13	5.9	61	0.4	96.47	1341	389.6	7.9	0.059	1.95	0.132	0.001	0.001	0.188	136.1	129.4	39	78.61	3175	5726
13	M14	6.8	79	4	68.7	1249	358.3	6.29	0.072	2.16	0.063	0.002	0.002	0.264	133.8	139.1	36	68.37	2661	4907
14	M16	7	78	2.4	6.46	155.5	6.48	0.64	0.057	0.183	0.09	0.001	0.002	0.17	108.29	36.22	57	116.3	189.9	620.1
15	M17	6.2	61	0.8	2.62	65.48	6.38	0.94	0.074	0.025	0.048	0.005	8E-04	0.044	81	81.43	45	91.22	47.92	398.5
16	M!8	7	64	0.8	4.44	95.24	2.02	0.8	0.142	0.107	0.124	0.008	8E-04	0.052	93	57.65	75	157.3	42.6	456.7
17	M19	7	68	1.2	3.91	92.86	2.46	0.87	0.104	0.084	0.072	0.005	3E-04	0.017	93	41.08	75	154.4	53.25	441.7
18	M20	7	69	1.4	16.13	546.7	277	2.76	0.106	0.093	0.105	0.005	0.001	0.049	77.03	138.7	15	33.31	1334	2517
19	M22	7	62	10	2.06	77.3	0.97	0.47	0.139	0.059	0.047	0.002	0.002	0.0145	71.945	19.08	64.5	138.2	32.18	304.9
20	M24	6.2	65	3	6.01	156.2	9.3	1.19	0.103	0.069	0.095	0.017	0.001	0.0575	106.95	22.83	67.5	123.4	192.4	564
21	M31	7.8	65	5	5.32	109.1	6.94	0,69	0,033	0,071	0,05	0.068	0.003	0.032	134.12	14.2	39.75	67.77	111.8	449.1
22	M33	7.5	65	28	38.8	1055	284	1.6	0.14	0.92	0.15	0.005	0.002	0.63	121.3	389.7		74.4	1789	3638
23	M36	8.1	77	5	7.2	181.2	9.8	0.5	0.11	0.05	0.06	0.008	0.002	0.05	98	37.8		71	273.3	2350
24	M53	7.5			6.2	173	11	0.44		0.11	0.15				78.5	63.5		161.5	198.5	650

TABLE 3: Some characteristics of Vietnam hot waters

No.	Sample	Ionic balance	Heat content (kJ/kg)	Chemical geothermometer			Minerals in deep water
				Quartz[1] (°C)	Chalc.[2] (°C)	Na/K[3] (°C)	
1	M01	-0.33	206.1			123.3	Anhy., Cal., Fluo.
2	M03	-12.93	180.8			105.0	Anhy., Cal., Fluo.
3	M04	-12.12	209.3			130.5	Anhy., Cal., Fluo.
4	M05	-7.73	157			108.5	Anhy., Cal., Fluo.
5	M06	15.13	242.7			127.8	Anhy., Cal., Fluo.
6	M07	8.65	272	127.9	100.0	114.8	Adu., Anhy., Mg.chlo., Flu., Cal., Micr., Sil-amor., Anac., Chan., Quar.
7	M08	-14.55	129.8			95	Anhy., Cal., Fluo.,
8	M09	7.12	226	124.8	96.7	150	Adu., Anhy., Albi., Cal.,Micr., Ana., Chan., Quar.,
9	M10	-1.39	272	132.5	105.1	154.1	Adu., Anhy., Alb., Cal., Fluo., Mic., Ana., Cha.,Quar.
10	M11	9.15	353.9	137.7	110.9	125.5	Adu., Anhy., Albi., Calci., Fluo., Anal.,Chan., Quar.
11	M12	16.46	326.5			108.2	Anhy., Cal., Fluo.,
12	M13	-13.74	255.3	155.4	130.5	166.3	Adu., Anhy., Albi., Cal., Fluo., Micr., Ana., Chal., Quar
13	M14	-5.61	330.7	153.2	128.1	141.4	Adu., Anhy., Cal., Fluo., Micr., Ana., Chan., Quar.
14	M16	-1.32	326.5	140.4	113.9	119.1	Adu., Anhy., Albi., Calc., Fluo., Micr., Ana., Chan., Quar.
15	M17	-16.07	255.3	125.8	97.7	116.1	Adu., Anhy., Albi., Cal., Fluo., Mic., Anal., Chal., Quar.
16	M18	7.34	267.8	133	105.7	128.7	Adu., Anhy., Albi., Cal., Fluo., Mic., Cha., Quar.
17	M19	7.68	284.6	132.3	104.9	120.4	Adu., Anhy., Albi., Cal., Fluo., Mic., Ana., Cha., Quar.
18	M20	-7.01	288.8	122.9	94.5	94.6	Adu., Anhy., Albi., Cal., Fluo., Mic., Ana., Cha.,Quar.
19	M22	14.94	259.5	119.3	90.6	89.1	Adu., Anhy., Albi., Cal., Fluo., Mic., Ana., Cha.,Quar.
20	M24	9.27	272	140.8	114.3	113.7	Adu., Anhy., Albi., Cal., Fluo., Mic., Ana., Cha.,Quar.
21	M31	19.3	272	151.9	126.7	132.7	Adu., Anhy., Albi., Cal., Fluo., Mic., Ana., Cha.,Quar.
22	M33	3.99	272	147.4	121.6	108.2	Adu., Anhy., Albi., Cal., Fluo., Mic., Ana., Cha., Quar.
23	M36	-3.71	322.3	133.7	106.5	116.0	Adu., Anhy., Albi., Cal., Fluo., Mic., Ana., Cha.,Quar.
24	M56	13.1		123.7	95.4	108.3	Adu., Anhy., Fluo., Si.amor., Cha.,Quar.

[1] Fournier and Potter, 1982 [2] Fournier, 1977 [3] Arnórsson et al., 1983

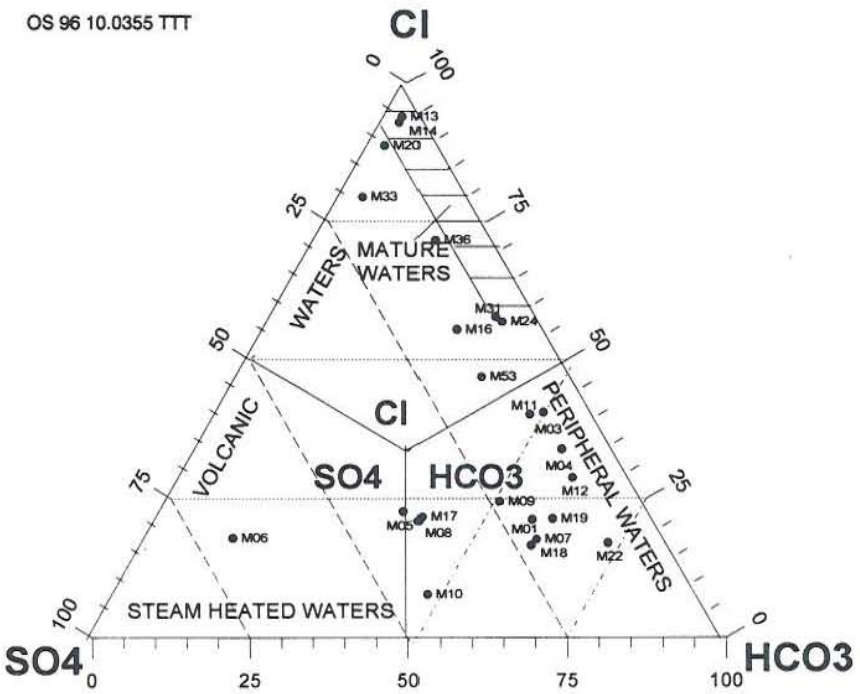

FIGURE 2: Cl-SO_4-HCO_3 diagram for thermal waters of 24 hot springs in the research area

For an initial classification, in terms of the major anions *Cl*, SO_4 and HCO_3, a triangular diagram (Giggenbach, 1991) was used (Figure 2). The position of a data point in this diagram is simply obtained by first finding the sum S of the concentrations C_i (in mg/kg) of all three constituents involved. In the present case

$$S = C_{Cl} + C_{SO_4} + C_{HCO_3} \tag{1}$$

The next step consists of the evaluation of %-*Cl*, %-SO_4 and %-HCO_3

$$\%-Cl = 100\, C_{Cl}/S \tag{2}$$

$$\%-SO4 = 100\, C_{SO_4}/S \tag{3}$$

and

$$\%-HCO3 = 100\, C_{HCO_3}/S \tag{4}$$

With the exception of the water from M06, which falls in the field of steam-heated waters, the waters belonged to two main groups. One group consists of samples M05, M01, M08, M17, M10, M18, M07, M22, M19, M09, M12, M04, M03, M11 which are peripheral waters, the others are mature waters (M13 and M14) or close to the field of mature waters.

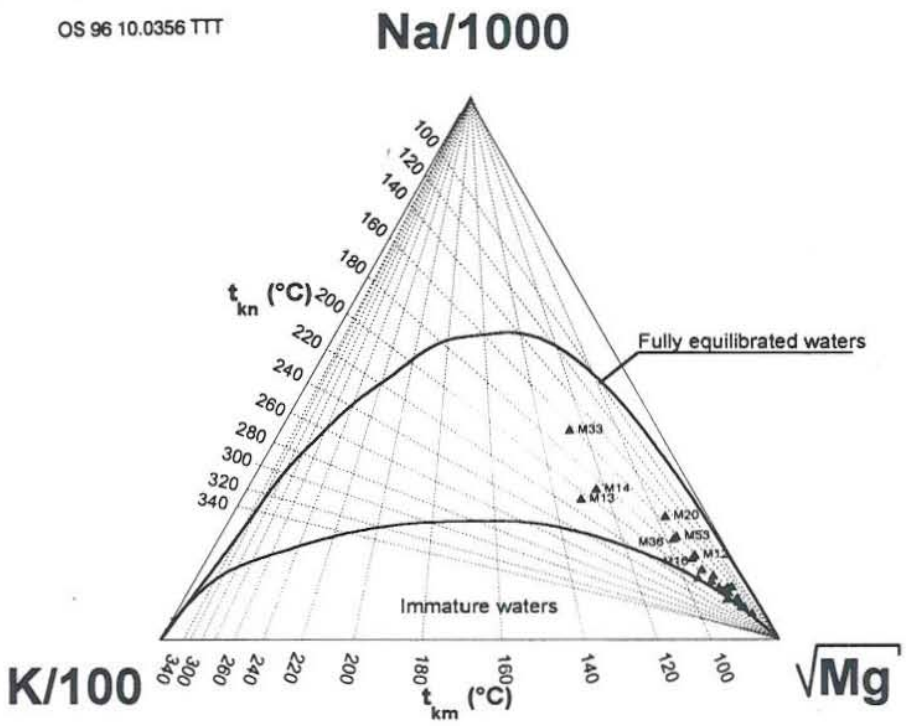

FIGURE 3: The Na-Kn Mg diagram for thermal waters of 24 hot springs in the research area

The Na-K-Mg triangular diagram (Giggenbach, 1991) is also obtained in analogous manner with the *Cl-SO_4-HCO_3* diagram and the position of a data point on the diagram is calculated similarly (Figure 3):

$$S = C_{Na}/1000 + C_K/100 + \sqrt{C_{Mg}} \quad (5)$$

$$\%-Na = C_{Na}/10S \quad (6)$$

$$\%-K = C_K/S \quad (7)$$

$$\%-Mg = 100\sqrt{C_{Mg}}/S \quad (8)$$

This diagram clarifies better the origin of the water. Corresponding waters were all shifted in the diagram. All waters plot in the field of partially equilibrated waters. They can be divided into two groups, one including samples M13, M14 and M33 is clustered close to the full equilibrium curve and the rest of the samples close to the $\sqrt{Mg}$ corner. The *Na/K* temperatures of the samples range from 150 to 210°C, but the *K/Mg* temperatures from 30 to 130°C.

The alkali metal probably least affected by secondary processes is *Li*. It may, therefore, be used as a "tracer" for the initial deep rock dissolution process and as a reference constituent to evaluate the possible origin of the other two important "conservative" constituents of thermal waters, *Cl* and *B*. The triangular diagram of *Cl-Li-B* (Giggenbach, 1991) is obtained in an analogous manner to the *Cl-SO_4-*

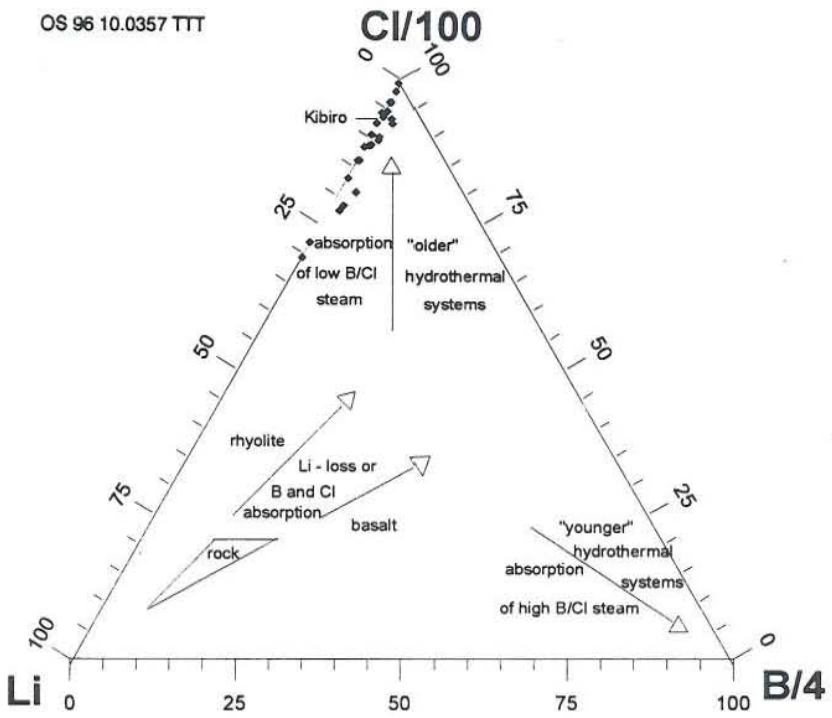

FIGURE 4: The Cl-Li-B diagram for thermal waters of 24 hot springs in the reasearch area

HCO_3 diagram. The position of a data point on the diagram is calculated (Figure 4):

$$S = C_{Cl}/100 + C_{Li} + C_B/4 \tag{9}$$

$$\%-Cl = C_{Cl}/S \tag{10}$$

$$\%-Li = 100\,C_{Li} \tag{11}$$

$$\%-B = 25\,C_B/S \tag{12}$$

According to this diagram, there are only two samples, M07 and M10, whose content are relatively low in comparison with the others, but it does not plot in the field of crustal rock composition. All samples are relatively rich in chloride, the concentrations plot on and near the axis *Li*-Cl/100 and close to the corner *Cl*/100. The initial compositions have been modified through the absorption of low *B/Cl* magmatic vapours, or affected by the admixture of low *B/Cl* seawater. The *B* content of geothermal fluids is likely to reflect, to some degree the maturity of a geothermal system. Because of their volatility, they are likely to be expelled during the early heating-up stages. Fluids from "older" hydrothermal systems can be expected to be depleted in this element.

The saturation state was calculated for those minerals that are calculated in the WATCH program (Bjarnason, 1994) and for which sufficient information is available. These minerals are listed in Table

3. In seven samples, saturation states of only three minerals could be calculated because of lack of analytical data. The chemical geothermometers used by this program, Na/K, quartz and chalcedony, and the results obtained are listed in Table 3. The average geothermometer temperatures for the samples fall in the range 95°C (sample M08) to 151°C (sample M13).

In contrast to using individual geothermometers, Reed and Spycher (1984) have presented a different approach to geothermometry. Their method is neither based on the assumption of predetermined mineral equilibrium nor the use of empirically calibrated geothermometers. It involves evaluating the saturation state of water of a specific composition with a large number of minerals at a particular temperature, at which the water has equilibrated. This method requires the calculation of the saturation index, log Q/K at different temperatures and the construction of a diagram of log Q/K versus temperature. When an aqueous solution has reached equilibrium with respect to a mineral, the ion activity product, Q, calculated from analytical results for the water sample should be the same as the solubility product K, i.e. $Q/K = 1$. This quantity may, however, vary by orders of magnitude, so it is more convenient to study the logarithm of the ratio, commonly called the saturation index, log Q/K, in which case an index value of zero denotes the equilibrium condition. If a water is supersaturated, the index is positive and the mineral has a tendency to precipitate. If the water is undersaturated, the index is negative, and the mineral has a tendency to dissolve. Moreover, the saturation index also reflects the temperature of the reservoir, at the point where the mineral curves in the water intersect at a certain temperature, ideally on the zero line. Now, if it is possible to calculate the activities of free ions from a given water analysis, then it is a relatively simple matter to calculate the index quantitatively. The method requires calculation of the aqueous speciation, gas pressure, activities and solubility products for the minerals at any temperature from 0 to 300°C. The program WATCH is used for this as well as to compute species concentrations, activity coefficents, activities and solubility products (Arnórsson et al., 1982, Bjarnason, 1994) for the minerals when the equilibrated fluids are allowed to cool conductively from the reference temperature to a lower temperature. The results of conductive cooling of the hot water from twenty-four hot springs at 20°C intervals from the reservoir temperature to measured temperatures at the surface were calculated. The index log Q/K for three minerals were calculated for seven samples and five to fifteen minerals for seventeen samples. The diagrams for the twenty-four samples are shown in Figure 5. The results can be grouped for certain temperature ranges, except for samples M-10 and M-53, for which a wide scatter is obtained (Table 4).

Mixing of ascending hot water with cold groundwater in shallow parts of hydrothermal systems, appears to be common. Mixing can also occur deep in hydrothermal systems, especially at the margins. The effects of mixing upon various geothermometers is discussed below.

When all the thermal waters reaching the surface at a given locality are mixtures of hot and cold water, recognition of that situation can be difficult. The recognition that mixing took place underground is especially difficult where water-rock re-equilibration has occurred after mixing. Complete or partial chemical re-equilibration is more likely if the temperature after mixing is well above 110-150°C or if mixing takes place in aquifers with long fluid residence times.

Under some circumstances the dissolved silica concentration of a mixed water may be used to determine the temperature of the hot water component (Fournier and Truesdell, 1974; Truesdell and Fournier, 1977). The simplest method of calculation uses a plot of dissolved silica vs. the enthalpy of liquid water. For example, in Figure 6a, there are two samples represented in the diagram as B and D. Because the cold water was not sampled and analyzed, point A is assumed to represent the hypothetical cold water (temperature: 25°C and SiO_2 35 ppm) in the study area. For the situation in which no steam is lost before mixing, plot the silica and heat contents (enthalpies) of cold water (A) and a mixture of geothermal (B) as two points, draw a straight line from A to B (B is a mixed water from a warm spring) to intersect the quartz solubility curve. Point C on this curve gives the silica content and enthalpy of the deep hot water component and its temperature is obtained from steam tables (e.g. Keenan et al., 1969).

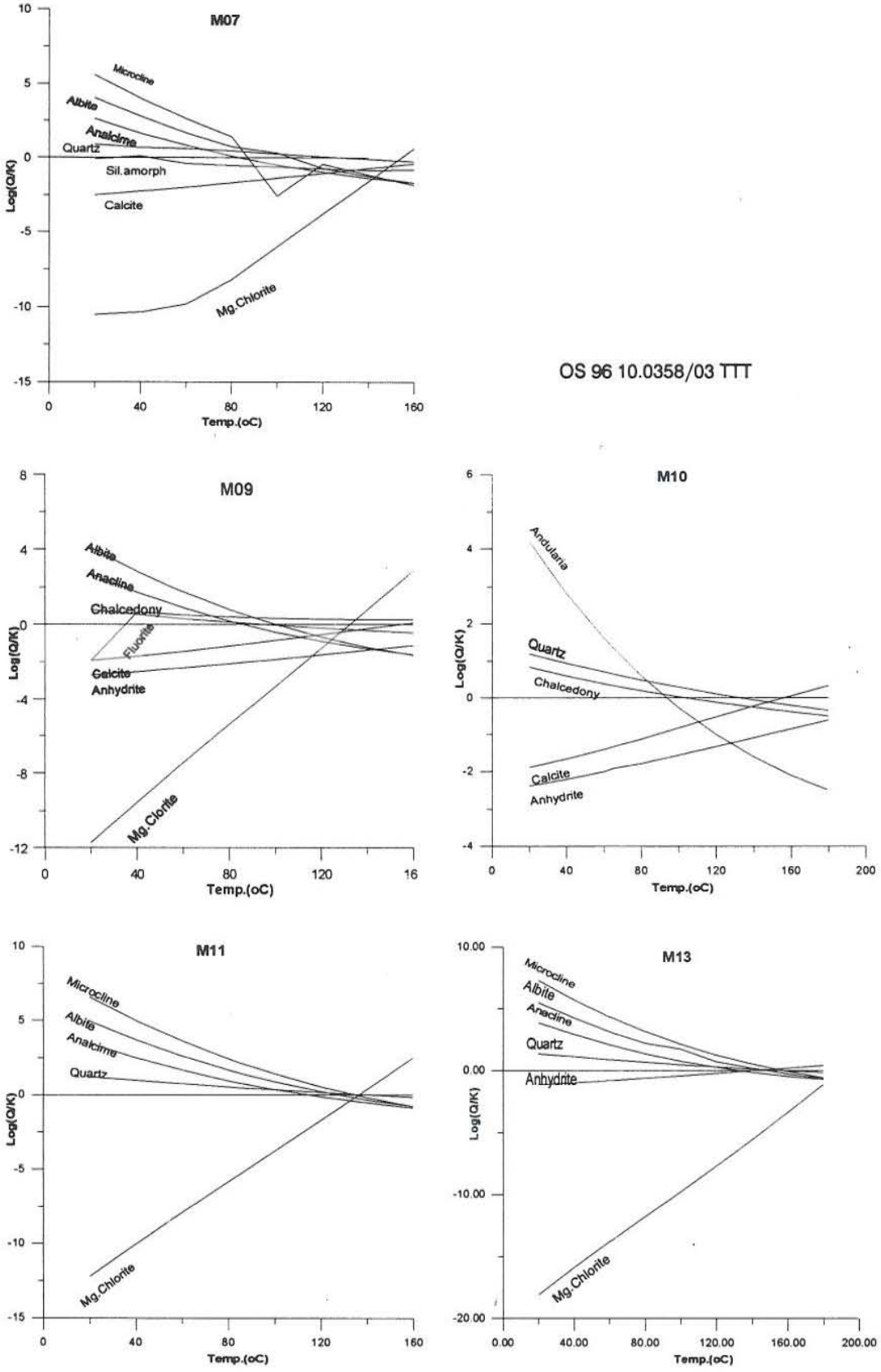

FIGURE 5: Mineral equilibrium diagrams for the thermal waters of 17 hot springs in research area

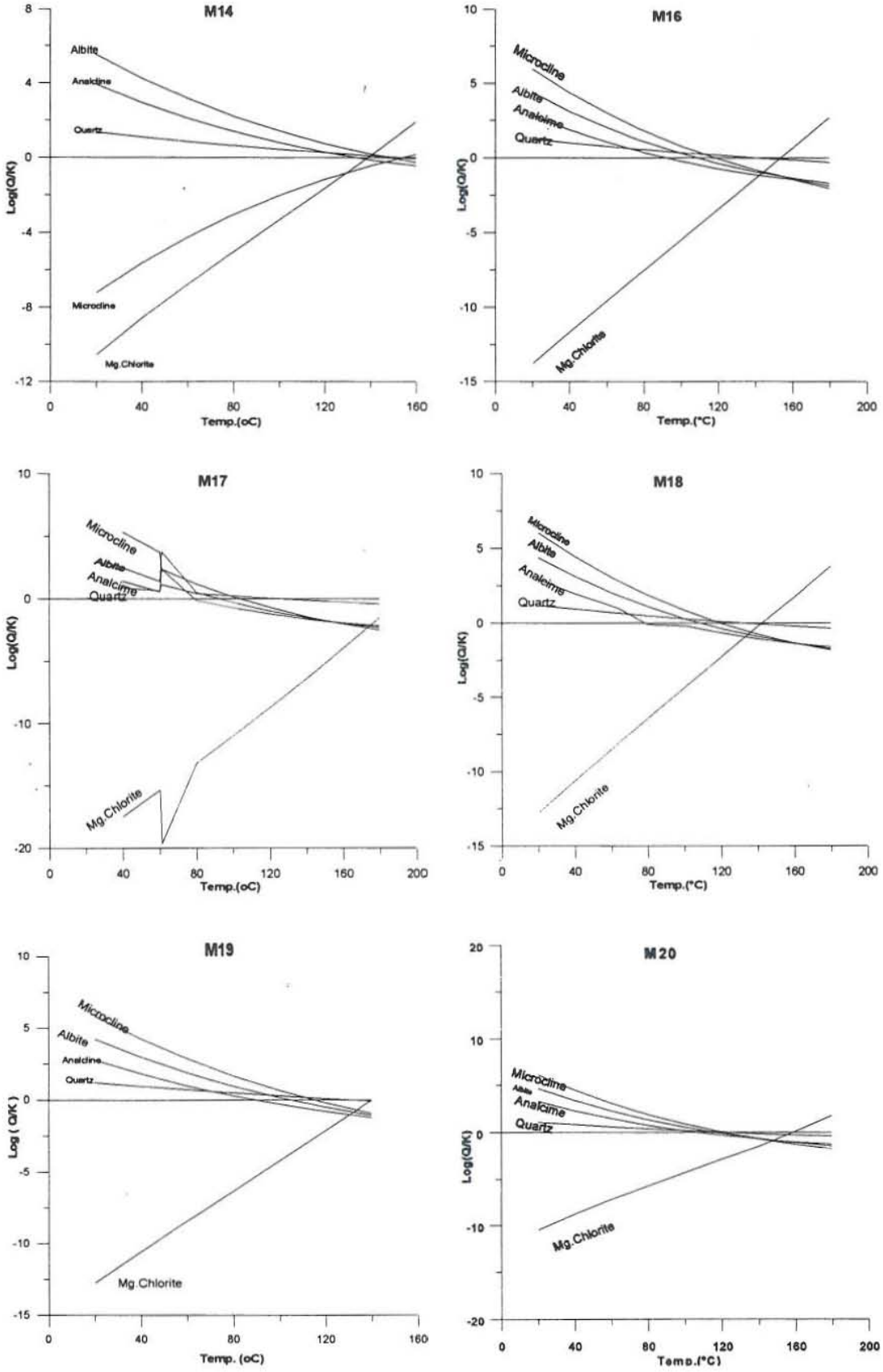

FIGURE 5: Mineral equilibrium diagrams for the thermal waters of 17 hot springs, continued

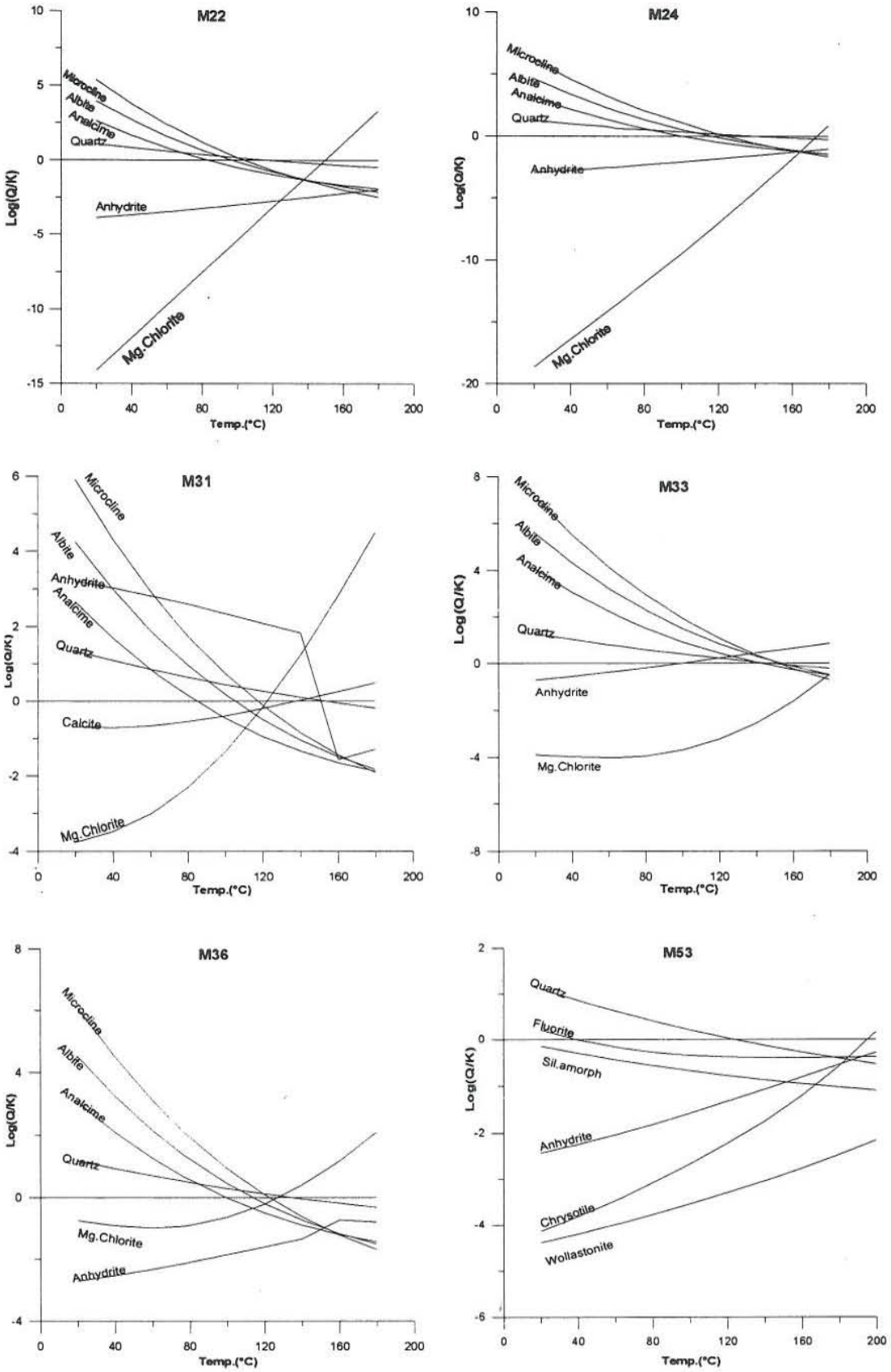

FIGURE 5: Mineral equilibrium diagrams for the thermal waters of 17 hot springs, continued

TABLE 4: Summary of the log *Q/K* results for 15 samples from the research area (see Figure 5)

Temperature range (°C)	Hot springs	Saturation minerals
80-110	M-07, M-09, M-22	Albite, analcime (all), microline, Quartz (07, 22)
90-130	M-24, M-36	Microline, albite, analcime, quartz (both), Mg-chlorite (36)
120-140	M-11	Microline, albite, analcime, quartz, Mg-chlorite
130-155	M-13, M-14, M-33	Microline, albite, analcime, quartz, Mg-chlorite

For the situation in which the maximum amount of steam is lost from the hot water before mixing plot the silica and heat contents of cold and warm spring waters as two points, A and D. Draw a straight line through these points and extend that line to the enthalpy of the residual liquid water at the assumed temperature of separation and escape of steam, 100°C; in this case, the residual liquid water before mixing will have an enthalpy of 419 kJ/kg (Point E). Move horizontally across the diagram from point E to the maximum steam loss curve, point F. The original silica concentration of the hot water component is given by point H. The original enthalpy of the hot water will lie at a value along the horizontal line, between F and G and the temperature is obtained from a steam table.

Such a diagram was prepared for sixteen samples, which could be divided into two groups according to the SiO_2 content. The first group with lower SiO_2 content (Figure 6b) was treated as if no steam were lost before mixing and the second group with higher SiO_2 content (Figure 6b) was treated as if a maximum amount of steam was lost before mixing. The silica-enthalpy mixing model temperatures for the samples are presented in Table 5 along with other results of chemical geothermometry, with a calculated average geothermometer temperature for each sample.

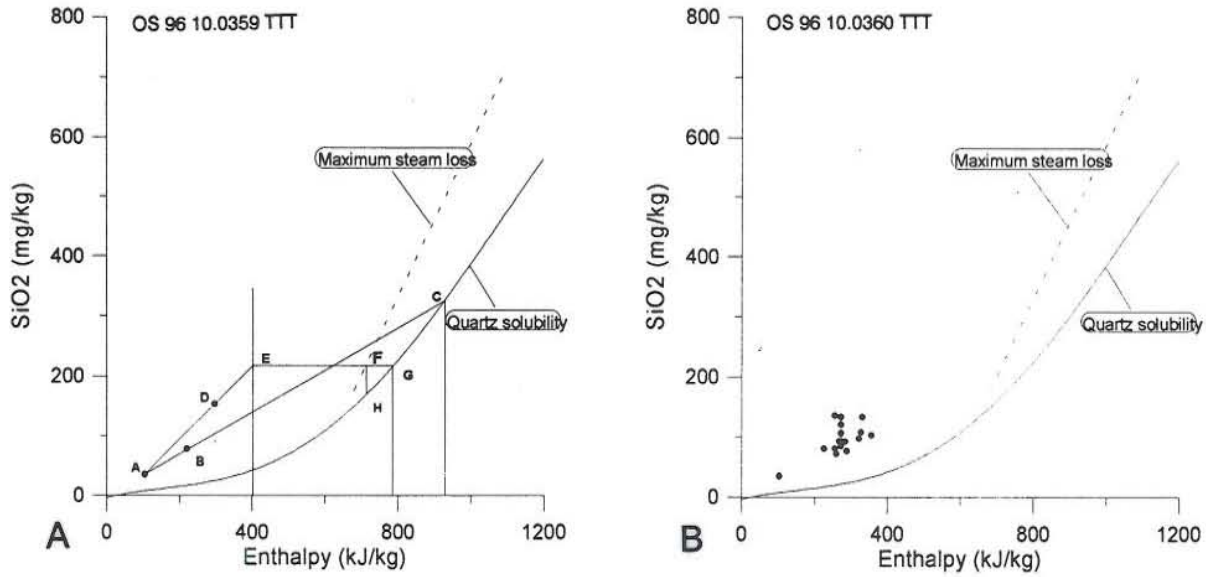

FIGURE 6: Dissolved silica-enthalpy diagram for determining the temperatures of hot water components mixed with cold water, a) An example of the use of the diagram with two samples; b) 16 samples from the reasearch area plotted on the diagram

TABLE 5: The calculated geothermometer temperatures for 24 thermal springs in the research area

No.	Sample	Temperature by Na-K-Mg (°C)		LogQ/K	Temperat. by mixing model	Average geothermometer temperature
		Na/K[1]	K/Mg[1]	(°C)[2]	(°C)[3]	(°C)
1	M01	160-200	40	130-160		123.3
2	M03	160-200	35	130-160		105.0
3	M04	160-200	30	130-160		130.5
4	M05	160-200	35	165-175		108.5
5	M06	160-200	50	130-160		127.8
6	M07	160-200	45	110-120		114.3
7	M08	160-200	45	130-160		95.0
8	M09	160-200	55	80-140	127.0	123.8
9	M10	160-200	53	80-140	131.0	127.2
10	M11	160-200	55	135	140.0	124.4
11	M12	210	65	130-160		108.2
12	M13	190	130	135-155	167	144.1
13	M14	160-200	122	130-150	154.0	140.9
14	M16	160-200	75	115-150	142.0	124.4
15	M17	160-200	60	90-175	137.0	113.2
16	M18	160-200	65	90-175	224.0	122.4
17	M19	160-200	48	100-135	142.0	119.2
18	M20	160-200	90	115-155	176.0	104.0
19	M22	170	90	100-165	137.0	99.7
20	M24	160-200	55	160	142.0	122.9
21	M31	160-200	60	115-160	169.0	137.1
22	M33	160-200	129	130-150	148.0	125.7
23	M36	160-200	95	120-155	139.0	118.7
24	M53	160-200	85	150-175	138.0	109.1

[1] Giggenbach et al., 1983 [2] Reed and Spycher, 1984 [3] Fournier, 1977

4. EVALUATION OF DATA

The data used in this report is from Quy (1996). From seventy hot springs, the author selected twenty four with the aim of selecting hot springs that should be evenly distributed over the study area.

In the field, sampling was carried out following the official procedures described in Paces (1991), but owing to a lack of sampling experience and shortage of equipment as well as pure chemicals, the samples were not in the perfect order the author had expected.

The surface temperatures of the hot springs were measured using a mercury thermometer and, consequently, the accuracy is quite questionable. The litmus paper used for measuring the pH of hot water is not a precise method. The flowrates were not properly measured. For SiO_2 determination in hot springs with temperatures above 65°C, distilled water was used for dilution in the proportion 1:10. The acid used for acidification was HCl 5M, but not pure. There are some hot springs with gas bubbles, i.e. gas flows were present which could not be sampled due to lack of equipment. The samples were

transported by car to the laboratory without any damage.

The samples were analyzed at the laboratory of the National Center of Natural Science and Technology of Vietnam. All the information recorded during sampling was conveyed to the analyst. The analytical methods were applied properly, and the results obtained were acceptable. Seven samples were not analyzed for SiO_2 and none for H_2S and NH_3 , though they are quite important for interpretation. The ionic balances obtained for the analytical results are acceptable for interpretation.

The lithology and mineralogy of the bedrocks at the sites of the hot springs were not studied properly. In general, the geological investigation was not detailed.

5. DISCUSSION AND CONCLUSIONS

In order to clarify the origin, features and nature of thermal springs as well as the temperatures of aquifers, the author has utilized geochemical methods to study twenty-four hot springs in the territory. In the study area, there are several types of bedrock such as basaltic rocks, metamorphic and terrigenous formations and so on. There are signs of intensive tectonic activity; many faults have been formed, which have facilitated the emergence of hot water. All the hot springs investigated are located in the coastal zone, 5-25 km from the sea.

The origins of the thermal springs are complicated. For the low salinity waters (usually with TDS of the order of 300-700 mg/kg), all dissolved chemicals derive from the interaction with the reservoir rocks under conditions of temperatures possibly not higher than 100-120°C. Six hot springs have TDS higher than 1000 mg/kg (M01, M13, M14, M20, M33, M36). The origin of chemicals in these relatively high salinity thermal waters can be explained by the hydrolysis of rock-forming minerals such as quartz, etc. Using the methods described in Chapter 3.2, the results suggest that the hot waters can be divided into five groups (Table 6).

TABLE 6: Types of geothermal water in the Quangnam-Danang - Baria-Vungtau area, Vietnam

Type of water	Sample no.
Mature or close to it	M13, M14, M16, M20, M24, M.31, M33, M36
Peripheral	M01, M03, M04, M07, M09, M11, M12, M18, M19, M22
Steam-heated	M06
Intermediate (mature-peripheral)	M53
Intermediate (peripheral-steam heated)	M05, M08, M10, M17

The full equilibrium curve in the diagram (Figure 3) is the one based on the Giggenbach et al. (1983) Na/K geothermometer which gives relatively high values at low temperatures. Many Na/K geothermometers have been developed and their results differ considerably, especially at low temperatures. The reason is that they are based on different mineral assemblages. As stated above, the Giggenbach et al. (1983) geothermometer usually gives the highest values, Truesdell's (1976) the lowest, and those of Arnórsson et al. (1983) and Fournier (1979) yield intermediate results. We have drawn a Na/1000-K/100-$\sqrt{Mg}$ diagram using Arnórsson et al's (1983) curve for three samples and M33 actually plots above the equilibrium curve. Therefore, the values due to Giggenbach's curve or some intermediate value might be more correct and that is why his methods are used here (Figure 3). All the samples except for sample M06 which is steam-heated water, plotted in the field of partially equilibrated waters and can be divided into two groups, one close to the fully equilibrated waters curve and the other group close to the $\sqrt{Mg}$ corner. So they may be mixed geothermal and cold groundwaters.

The temperatures read from Figure 3 are Na-K and Mg-K. As mentioned above, Giggenbach's Na-K geothermometer tends to give relatively high results at such low temperatures compared to other Na-K geothermometers. The Mg-K geothermometer is extremely quick to respond to temperature changes and usually reflects a very recent temperature, quite often the surface temperature of the spring. For instance, from the diagram we see for three samples that Arnórsson's et al. (1983) Na-K geothermometer results in a temperature close to 160°C, but Giggenbach's about 210°C for sample M13. The Mg-K temperature on the other hand gives about 130°C which can be regarded as a minimum.

Referring to the Cl/100-Li-B/4 diagram (Figure 4), all samples fall near the Cl-Li axis and close to the Cl corner. These waters are modified through absorption of low B/Cl magmatic vapour or affected by the admixture of low B/Cl seawater. Samples M06 and M09 may, however, be slightly less affected by magmatic steam and/or seawater.

The log Q/Ks for minerals in hot waters were calculated using the program WATCH and plotted versus temperature. There are seven diagrams which are based on such calculations for only three minerals, i.e. for M01, M03, M04, M05, M06, M08 and M12, and suggest temperatures in the range 130-160°C for these waters. Sample M07, for which most curves intersect slightly below the zero line in the temperature range 110-120°C, can be interpreted as a deep fluid at about that temperature, which is mixed with a small amount of cold groundwater before emerging in a spring. The intersections for mineral M09 are scattered in the range 80-140°C, the higher temperatures probably being due to a deep fluid which is coming up fairly slowly, getting mixed with cold groundwater and re-equilibrating with some minerals before emerging. M10 is probably similar, but M11 appears to show a single deep water temperature of 135°C. M13 also shows a single deep water in the temperature range 135-155°C. Similarly, M14 is in the temperature range 130-150°C. For M16, most of the curves intersect each other slightly below the zero line in the temperature range 115-150°C, which would be interpreted as a deep fluid at about that temperature which is mixed with a small amount of cold groundwater before emerging in a spring. M17 is in the range 90-175°C, the higher temperature being due to a deep fluid which is coming up re-equilibrating with some minerals before emerging in a spring. M18 is probably similar, but for M19 all the curves intersect slightly below the zero line in the temperature range 100-135°C, which would be interpreted as deep fluid at about that temperature, mixed with a small amount of cold groundwater before emerging in a spring. M20 is probably similar in a temperature range 115-155°C. The higher temperature may be due to a deep fluid coming up slowly. For M22, almost all the curves intersect below the zero line in the temperature range 100-165°C, the higher temperature probably being due to a deep fluid which is coming up slowly, getting mixed with cold groundwater and re-equilibrating with some minerals before emerging. For M24, all the curves intersect slightly below the zero line at temperature 160°C and probably mixed with a small amount of cold groundwater before emerging in a spring. The mineral curves for M31 are scattered in the range 115-160°C, maybe due to a fluid which is coming up fairly slowly and mixing with a small amount of cold water. For M33, most curves intersect slightly below the zero line in the temperature range 130-150°C which would be interpreted as a deep fluid at about that temperature mixed with a small amount of cold groundwater before emerging in a spring. M36 is similarly in the temperature range 120-155°C, the higher temperature being due to a deep fluid coming up fairly slowly and getting mixed with very small amount of cold groundwater before emerging in a spring. Values for M53 are scattered in the range 150-175°C, the higher temperature being due to a deep fluid which comes up slowly and mixes with a small amount of cold groundwater before emerging in a spring.

The author also utilized the SiO_2 mixing model, assuming that the waters are cooling conductively, i.e. the diagram showing SiO_2 concentration versus heat content (enthalpy) for the samples in which SiO_2 was analysed. The temperatures obtained, using this method, are slightly higher than from the geothermometers except for sample M18 whose temperature is found to be 100°C, or slightly lower than obtained from the plot of log Q/K versus temperature. So the temperatures resulting from

geothermometers which were calculated by the WATCH program may be considered as average temperatures.

Finally, a summary of aquifer temperatures of hot springs which were calculated by the above methods, is presented in Table 5. The highest estimated geothermometer temperature is 141°C (sample M13), but all the springs could be divided into two groups, low-enthalpy (<125°C) and medium-enthalpy (125-150°C) springs.

6. RECOMMENDATIONS ON DETAILED GEOTHERMAL EXPLORATION OF THE AREA

In conclusion, detailed exploration of the geothermal potential of the area is needed as follows:

1. It is necessary to carry out geophysical soundings across the area.

2. Samples, including gas and steam samples from hot springs where gas flows were observed, need to be collected.

3. The sampling procedures should be standard and the equipment should be adequate for collecting samples.

4. Analysis for stable isotopes which help to assess the age and origin of hot water should be carried out on samples from selected hot springs.

5. The prospective thermal springs studied should be investigated in more detail in order to estimate their potential for energy production.

ACKNOWLEDGEMENTS

I would like to acknowledge the Government of Iceland and the United Nations University for giving me the opportunity to study all necessary aspects and develop this report, to Dr. Ingvar Birgir Fridleifsson for his selection of myself to attend the 1996 Geothermal Training Course and for all his help during the course, and to Mr. Lúdvík S. Georgsson and Mrs. Gudrún Bjarnadóttir for their special help and guidance throughout the training period. My thanks to Dr. Halldór Ármannsson, my supervisor, for sharing with me his experience and knowledge of geochemistry and guiding me in completing the report. Also, my thanks to all lecturers and staff members at ORKUSTOFNUN for their help and willingness to share their knowledge and experience and to all the fellows for their friendship and company.

I am also indebted to Dr. Ho Vuong Binh and Mr. Hoang Huu Quy from the Research Institute of Geology and Mineral Resources of Vietnam for their help and for providing me with the data used here. To all members of my family and friends who gave me spiritual inspiration for my stay in Iceland, I say thank you so much and God bless you all.

REFERENCES

Arnórsson, S., Gunnlaugsson, E., and Svavarsson, H., 1983: The chemistry of geothermal waters in Iceland III. Chemical geothermometry in geothermal investigations. *Geochim. Cosmochim. Acta, 47,* 567-577.

Arnórsson, S., Sigurdsson, S., and Svavarsson, H., 1982: The chemistry of geothermal waters in Iceland I. Calculation of aqueous speciation from 0°C to 370°C. *Geochim. Cosmochim. Acta, 46,* 1513-1532.

Bjarnason, J.Ö., 1994: *The speciation program WATCH, version 2.1.* Orkustofnun, Reykjavík, 7 pp.

Fournier, R.O., 1977: Chemical geothermometers and mixing models for geothermal systems. *Geothermics, 5,* 41-50.

Fournier, R.O., 1979: Geochemical and hydrologic considerations and the use of enthalpy-chloride diagrams in the prediction of underground conditions in hot spring systems. *J. Volc. & Geoth. Res., 5,*1-6.

Fournier, R.O., and Potter R.W.II, 1982: A revised and expanded silica (quartz) geothermometer. *Geoth. Res. Council Bull., 11-10,* 3-12.

Fournier, R.O., and Truesdell, A.H., 1974: Geochemical indicators of subsurface temperature. Part 2, estimation of temperature and fraction of hot water mixed with cold water. *U.S. Geol. Survey J. Res , 2,* 263-270.

Gianelli, G., Piovesana, F., and Quy, H.H., 1996: Reconnaissance geochemical study of thermal waters of South and Central Vietnam. *Geothermics, submitted.*

Giggenbach, W.F., 1991: Chemical techniques in geothermal exploration. In: D'Amore, F. (coordinator), *Application of geochemistry in geothermal reservoir development.* UNITAR/UNDP publication, Rome, 119-142.

Giggenbach, W.F., Gonfiantini, R., Jangi, B.L., and Truesdell, A.H., 1983: Isotopic and chemical composition of Parbati Valley geothermal discharges, NW-Himalaya, India. *Geothermics, 12,* 199-222.

Keenan, J.H., Keyes, F.G., Hill, P.G., and Moore, J.G., 1969: *Steam tables (International edition - metric units).* John Wiley, N.Y. 162 pp.

Nghiep, V.C., 1986: Geothermal resources in Vietnam and the neighbouring countries and perspectiveness of their use for energy purpose. *Proceedings of the 1st Conference on Geology of Indochina.* Hanoi,Vietnam.

Paces, T. (editor), 1991: *Fluid sampling for geothermal prospecting.* UNITAR/UNDP publication, Rome, 93 pp.

Quy, H.H., 1996: *General evaluation of geothermal potential in the tectonic setting of Vietnam.* Geoth. Res. Council., Bulletin, 25-2, 63-76.

Reed, M.H., and Spycher, N.F., 1984: Calculation of pH and mineral equilibria in hydrothermal waters with application to geothermometry and studies of boiling and dilution. *Geochim. Cosmochim. Acta, 48,* 1479-1490.

Tri, T.T., et al. 1986: *Tectonics of Vietnam. The explanatory text for the tectonic map of Vietnam, scale, 1:1,000,000*. Geological Survey of Vietnam, Hanoi, Vietnam.

Truesdell, A.H., 1976: Summary of section III - geochemical techniques in exploration. *Proceedings of the 2nd U.N. Symposium on the Development and Use of Geothermal Resources, San Francisco, 1,* liii-lxxix.

Truesdell, A.H., and Fournier, R.O., 1977: Procedure for estimating the temperature of a hot water component in a mixed water using a plot of dissolved silica vs. enthalpy. *U.S. Geol. Survey J. Res., 5,* 49-52.